The Cerebellum
https://doi.org/10.1007/s12311-020-01205-8

ORIGINAL ARTICLE

Longitudinal Analysis of the Relation Between Clinical Impairment and Gray Matter Degeneration in Spinocerebellar Ataxia Type 7 Patients

Anabel Contreras[1] · Gabriel Ramirez-Garcia[2] · Amanda Chirino[3] · Consuelo Morgado-Valle[1] · Erick H. Pasaye[4] · Carlos Hernandez-Castillo[5] · Rosalinda Díaz[3] · Juan Fernandez-Ruiz[3,6] · Luis Beltran-Parrazal[1]

Accepted: 13 October 2020

Abstract

Spinocerebellar ataxia type 7 (SCA7) is a neurodegenerative disease characterized by progressive ataxia and retinal degeneration. Previous cross-sectional studies show a significant decrease in the gray matter of the cerebral cortex, cerebellum, and brainstem. However, there are no longitudinal studies in SCA7 analyzing whole-brain degeneration and its relation to clinical decline. To perform a 2-year longitudinal characterization of the whole-brain degeneration and clinical decline in SCA7, twenty patients underwent MRI and clinical evaluations at baseline. Fourteen completed the 2-year follow-up study. A healthy-matched control group was also included. Imaging analyses included volumetric and cortical thickness evaluation. We measured the cognitive deterioration in SCA7 patients using MoCA test and the motor deterioration using the SARA *score*. We found statistically significant differences in the follow-up compared to baseline. Imaging analyses showed that SCA7 patients had severe cerebellar and pontine degeneration compared with the control group. Longitudinal follow-up imaging analyses of SCA7 patients showed the largest atrophy in the medial temporal lobe without signs of a progression of cerebellar and pontine atrophy. Effect size analyses showed that MRI longitudinal analysis has the largest effect size followed by the SARA scale and MoCA test. Here, we report that it is possible to detect significant brain atrophy and motor and cognitive clinical decline in a 2-year follow-up study of SCA7 patients. Our results support the hypothesis that longitudinal analysis of structural MRI and MOCA tests are plausible clinical markers to study the natural history of the disease and to design treatment trials in ecologically valid contexts.

Keywords SCA7 · Rate of atrophy · Effect size · Cognitive assessment · Motor deterioration

Anabel Contreras, Gabriel Ramirez-Garcia and Amanda Chirino contributed equally to this work.

Supplementary Information The online version contains supplementary material available at https://doi.org/10.1007/s12311-020-01205-8.

✉ Juan Fernandez-Ruiz
jfr@unam.mx

✉ Luis Beltran-Parrazal
lubeltran@uv.mx

[1] Centro de Investigaciones Cerebrales, Universidad Veracruzana, Berlin 7, Fracc. Monte Magno, C.P. 91193 Xalapa, Veracruz, Mexico

[2] Unidad Periférica de Neurociencias, Facultad de Medicina, Universidad Nacional Autónoma de México, Instituto Nacional de Neurología y Neurocirugía "Manuel Velasco Suárez", Mexico City, Mexico

[3] Laboratorio de Neuropsicología, Departamento de Fisiología, Facultad de Medicina, Universidad Nacional Autónoma de México, Coyoacán, C.P. 04510 Mexico City, Mexico

[4] Magnetic Resonance Unit, Institute of Neurobiology, Universidad Nacional Autónoma de México campus Juriquilla, Querétaro, Mexico

[5] CONACyT - Instituto de Neuroetología, Universidad Veracruzana, Xalapa, Veracruz, Mexico

[6] Facultad de Psicología, Universidad Veracruzana, Xalapa, Veracruz, Mexico

Published online: 12 November 2020

Introduction

Spinocerebellar ataxia type 7 (SCA7) is a neurodegenerative autosomal dominant inheritance disorder [1]. It is caused by an abnormal expansion of cytosine-adenine-guanine (CAG) triplet in the ATXN7 gene located in the chromosome 3p12-p21 [2, 3]. The abnormal expansion of CAG triplets leads to the expression of a mutant form of the protein ataxin-7 with several repetitions of glutamine. Clinically SCA7 is characterized by dysarthria, dysphagia, gait ataxia, and blindness due to pigmentary retinal degeneration [1, 4–6]. Studies that include cognitive testing show deficits in attention, verbal memory, and semantic fluency [7, 8]. Brain atrophy associated with SCA7 includes neuronal loss in specific areas spread across all cortical lobes, as well as in several subcortical regions including the cerebellum, the inferior olivary complex, the subthalamic nucleus, the pallidum, and the substantia nigra [9, 10].

A small number of longitudinal studies have characterized neurodegeneration in spinocerebellar ataxias such as SCA1, SCA3, and SCA6 and its relation to clinical deterioration. These studies have used structural neuroimaging analyses combined with motor scales such as the Scale for the Assessment and Rating of Ataxia (SARA), Inventory of Non-Ataxia Symptoms, Spinocerebelar ataxia functional index, and Unified Huntington's Disease Rating Scale [11]. However, there is only one longitudinal study involving SCA7 patients that analyzed pons and cerebellar volumes in comparison with other SCAs (SCA1, SCA2, and SCA3) [10]. It also explored the relation of the progression of cerebellar and pontine degeneration with the decline in SARA and the Composite Cerebellar Functional Severity Score (CCFS). Nonetheless, the authors did not report significant changes in SARA scores, or specific correlations between structural decline and clinical scores in SCA7.

In order to expand our knowledge on the neurodegenerative changes occurring in SCA7 patients, here we aimed to characterize longitudinally whole brain atrophy and motor and cognitive function during a period of 2 years. First, we performed a neuropsychological test battery, SARA scale, and MRI scanning in a cohort of SCA7 patients and an age-, gender-, and years of schooling-matched group of healthy control subjects. We found statistically significant changes in the Mini-Mental State Examination (MMSE) and the Montreal Cognitive Assessment (MoCA) scores and a conspicuous atrophy of the cerebellum and pons. Furthermore, the MoCA score and SARA scale also showed a significant decline over time, and structural MRI analyses showed atrophy in the medial temporal lobe, without signs of progression of cerebellar and pontine atrophy in SCA7 patients. We suggest that longitudinal studies using the SARA scale, MoCA test, and structural MRI can potentially be used as both progression and treatment response markers in treatment trials.

Material and Methods

Participants

Twenty SCA7 patients with molecular diagnosis were initially enrolled in the study. However, after completing the initial testing, six of them did not participate in the second testing 2 years later. Reasons for drop-out included the progression toward advanced stages of the disease in five patients showing extreme ataxia that precluded MRI scanning, and the passing of one patient. The remaining SCA7 group consisted of 5 females and 9 males. We also included subject-to-subject–matched healthy participants to SCA7 patients (age-, gender-, and years of schooling-matched) as a control group. This group consisted of 14 volunteers (5 females, 9 males) with no history of neurological injury or psychiatric diseases. For the longitudinal evaluation, only 12 healthy control completed the follow-up assessment since two declined to further participate in the study.

Patients and healthy controls underwent the same standard neuroimaging procedures, as well as two sets of clinical and cognitive assessments (baseline and follow-up) with a mean inter-assessment interval of 23.83 months (SD 0.44 months) for patients and 26.25 months (SD 1.28 months) for healthy controls. All participants were native Spanish speakers recruited from the central region of Veracruz, México. The Research and Ethics committee of the Faculty of Medicine of the Universidad Nacional Autónoma de México approved the study. Written informed consent was obtained from each participant according to the Helsinki declaration (World Medical Association, 2013).

Motor Assessment

All participants underwent ataxia evaluation using SARA that includes eight tests: gait, stance, sitting, speech disturbance, finger-chase test, nose finger test, fast alternating movements test, and heel-shin test, with total score ranging from 0 (no ataxia) to 40 (severe ataxia) [12]. However, in order to avoid a bias in the total score due to the fact that some SCA7 patients have visual deficiencies, we eliminated the nose finger and the finger-chase test from the original test getting a total score range from 0 to 32.

The PATA test was administrated to assess articulatory speed [13]. Participants were asked to repeat "pata" as quickly and distinctly as possible for 10 s. The test was repeated twice and the mean number of correct "pata" words spoken by each participant was calculated.

Cognitive Assessment

The neuropsychological tests used were chosen for their minimal reliance on visual and motor performance.

Screening Tests

MoCA (blind version) screens different cognitive domains including memory, visuospatial abilities, attention, concentration and working memory, language, abstract reasoning, and orientation to time and place [14]. The maximum score is 22 points; a score above 18 is considered normal. MMSE consists of a variety of questions, grouped into 7 categories representing different cognitive domains including time and place orientation, verbal memory, attention and calculation, working memory, language, and visual construction [15]. Items 9 and 11 were eliminated from the total score for both groups due to the visual impairments of SCA7 patients (total score, 28).

Backward Digit Span

The backward digit span task measures the capacity to recall digits in reverse order. The examiner says a list of digits at a rate of approximately one digit per second. Subjects are required to immediately repeat the list in the inverse order. If they succeed after two opportunities, a list one digit longer is presented. The list length is gradually increased, starting with two numbers, to a maximum of nine items. The span is the length of the longest list recalled correctly [16].

Rey Auditory Verbal Learning Test Spanish Version

RAVLT-S examines auditory-verbal memory and learning strategies for lists of nouns presented verbally [17]. A 15-noun list (list A) is presented five times, and after each time the participants has to repeat as many words as possible. After an interference trial (list B), there is an immediate recall, a delayed recall (after 20 min) and a final trial of recognition of the list A nouns from a list of words that included nouns from list B plus 14 distractor nouns. Based on RAVLT-S performance, the following scores were calculated: immediate memory span, defined as total correct words recalled in the first trial (A1); learning rate, defined as the gain of recalled nouns over five trials; proactive interference, defined as the interference effect of a list of nouns previously learned over the learning of a new list; retroactive interference, defined as the interference effect of learning a new list of nouns over and old list previously learned; forgetting rate, defined as the loss of information acquired after 20 min; and recognition memory, defined as the percentage of nouns that were correctly identified as familiar from a list containing familiar and unfamiliar nouns. The learning curve was also analyzed as the total number of words recalled at each trial (A1 to A5) [18].

Verbal Fluency Tasks

In phonemic and semantic verbal fluency tasks, participants are asked to generate in 1 min as many words as possible that began with the letters P, M, R for phonemic fluency, and as many animal names as possible for semantic fluency. The qualitative analyses of the verbal fluency tasks were conducted using the Spanish adaptation of the verbal fluency scoring criteria previously reported [19]. The following measures were derived from these tasks: (1) total correct words, defined as the sum of all words produced minus repetitions and errors; (2) number of clusters, for semantic fluency successful semantic cluster consisted of three or more successive words within the same subcategory, e.g., farm animals, pet animals, water animals, and amphibians. For phonemic fluency, successful phonemic clusters consisted of three or more successive words that rhyme, begin with the same two letter or be homonyms. (3) A number of switches are defined as the number of transitions between clustered or non-clustered words (single words). (4) A mean cluster size is defined as the sum of all clustered words divided by the total number of clusters.

Depression Assessment

The Spanish version of the Center for Epidemiologic Studies Depression Scale (CES-D) was used as an indicator of depressed mood. A score above 16 was considered clinically significant [20].

MRI Data Acquisition and Analysis

Image Acquisition

All images were acquired with a 3 Tesla General Electric MR750 Discover system at the Instituto de Neurobiología of the Universidad Nacional Autónoma de México in Juriquilla, Querétaro, México. The study consisted in the acquisition of T1-3D anatomical high-resolution images using a SPGR sequence (Spoiled Gradient Recalled), with a TE/TR 3.18/8.16 ms; FOV 256×256 mm^2, and an acquisition and reconstruction matrix of 256×256, resulting in an isometric resolution of $1 \times 1 \times 1$ mm^3. MRI images were acquired at baseline and at follow-up 24 ± 0.70 months later. Image acquisition included non-replacement of MRI scanners during the longitudinal study, no relevant hardware or software changes, and no significant changes of images quality. All images were preprocessed before the analyses, including MNI orientation, denoising, and intensity inhomogeneity correction [21, 22].

Cross-sectional and Longitudinal Gray Matter Density Change Analysis

The structural analysis of the gray matter between control and SCA7 groups was performed using Voxel Based Morphometry (VBM) [23] implemented on FSL software (FMRIB Software Library; https://fsl.fmrib.ox.ac.uk/fsl/fslwiki/FSLVBM) [24]. First, we ran the Brain Extraction

Tool (BET) [25] for automatic brain extraction in each image to remove voxels from the scalp tissue, the skull, and dural venous sinuses [26]. Resulting images were segmented into gray matter, white matter, and cerebrospinal fluid (CSF) [24]. The next preprocessing step was spatial normalization of gray matter images from all participants, which involves transforming all subject's data to the ICBM 152 atlas of the Montreal Neurological Institute (MNI 152) [26] to create a study-specific template averaging normalized gray matter images. Then, the 28 native gray matter images were co-registered to this study-specific template through a non-linear co-registration, and local changes in expansion or contraction were corrected through a process known as modulation [26]. Smoothing was applied with an isotropic Gaussian kernel with a sigma of 3 mm prior to performing the voxel-wise tests. For cross-sectional analysis, we ran a no paired *t* test analysis between control and SCA7 groups initial testing data using the general linear model (GLM) and the randomize permutation method adjusted for multiple comparisons (10,000 permutations) [27]. Only the voxels showing a $p < 0.05$ corrected were considered significant. Longitudinal gray matter changes were examined using a flexible factorial design assessing time (baseline and follow-up) × groups (healthy control and SCA7) using the GLM and running 10,000 permutations. Significance correction was set at $p < 0.05$. Only clusters with a size of minimum 20 voxels were reported for the cross-sectional analysis. The significant clusters were segmented considering their local maxima values and binarized for visualization purposes. Each binary mask was applied to the single 4D modulate GM image of SCA7 group at baseline and follow-up. The correspondent values obtained were used to determine the cluster longitudinal effect size. Coordinates are reported in the standard anatomical space of the Montreal Neurological Institute (MNI) atlas for both analyses.

Longitudinal Cortical Thickness and Volume Analysis

Cortical reconstruction processing was performed using FreeSurfer software stable version 6.0.0 (http://surfer.nmr.mgh.harvard.edu/). All images from healthy controls and SCA7 (baseline and follow-up) were preprocessed independently following these steps: motion correction, nonuniform intensity correction, automated Talairach transformation, skull stripping, tissue partition, surface reconstruction by triangular tessellation, surface inflation, spherical mapping to standard coordinate system, as well as parcellation of cerebral cortex [28–36]. Resulting images were inspected for accuracy and minor manual corrections were performed. For longitudinal analysis, images were subsequently run through the longitudinal stream [36] and an unbiased within-subject template space and image (base) was created [37] for each SCA7 subject using robust and inverse consistent registration [38]. Skull stripping, Talairach transforms, atlas registration, spherical surface maps, and parcellations were initialized using common information from the within-subject template, significantly increasing reliability and statistical power [39, 40]. Cortical thickness and volume values resulting from this analysis were used to evaluate longitudinal gray matter change in SCA7 and their rate of change.

Statistical Analyses

Normality of the standardized residuals (for cognitive and motor variables) was evaluated with the Shapiro-Wilk test and by the quantile-quantile plot of each variable versus a normal distribution. Age, years of schooling, and months among evaluations were compared between patients and controls using independent samples Student's t test or Mann-Whitney *U* test, as appropriate. The effect sizes were calculated by Cohen's *d* or *r* scores.

Longitudinal changes of the SARA scale, PATA test, and neuropsychological assessment (except verbal fluency) were determined with independent two-way mixed ANOVAs using time (baseline and follow-up) as within-subjects factor and group (SCA7 and control group) as between-subjects factor. To compare patients and controls changes in the RAVLT-S learning curve, a three-way mixed ANOVA was conducted using time and trials (A1 to A5) as a within-subjects factor and the group as a between-subjects factor.

Significant interaction effects were further analyzed with post hoc pairwise comparisons using Bonferroni adjustment. Skewed distributions (SARA, CES-D, backward digit span, MMSE, and RAVLT-S retroactive interference) were log10 transformed before statistical analysis. The effect size was calculated by partial eta-squared (η_p^2).

Longitudinal changes on measures of verbal fluency were compared among groups with a linear mixed model (maximum likelihood estimation) for each variable. To control the influence of articulation deficits in verbal fluency tasks, PATA grand-mean centered scores were used as a time-varying covariate. The effect of the group (patients/controls) on the rate of change across time was tested in two growth parameters (initial status and linear slope), which were allowed to vary across individuals. A dichotomous variable (controls coded as − 1 and patients coded as 1) was created as a major predictor. Measures derived from verbal memory tests (RAVLT-S and backward digit), verbal fluency tasks, cognitive screening tests (Moca and MMSE) and motor tests (SARA and Pata), as well as the regional brain volumes at baseline, were corrected for multiple comparisons using FDR ($q = 0.05$). The aforementioned statistical analyses were conducted with SPSS 25 and statistical significance was set at $p < 0.05$.

Atrophy rate was calculated as the percentage of change relative to the baseline of the ROI volume estimated from automated segmentation and corrected for visit interval [11,

40]. This atrophy rate was computed for volume and cortical thickness measurements. The same formula was used to determine the clinical and neuropsychological rate of change of all the motor and cognitive scores.

$$\text{Percent change} = \frac{\left(\frac{\text{Follow-up ROI value} - \text{Baseline ROI value}}{\text{Baseline ROI value}}\right)}{\text{Visit interval(months)}}$$

The magnitude of the association between brain atrophy rate and motor and cognitive rate of change on the different measures used was determined through Spearman correlation. Statistical analyses were performed using R3.5.2 and RStudio 1.1.453 version with an alpha set at 0.05 as a statistical threshold for significance. FDR correction was employed to adjust for multiple analyses ($q = 0.05$).

In order to be able to compare with previous reports and between scales, we obtained effect size indices as previously suggested [11]. These were calculated as the mean score change/standard deviation (SD) of score change. Values of 0.20, 0.50, and 0.80 were considered to represent small, moderate, and large changes.

Results

Significant effects found for log10 transformed motor/cognitive scores (SARA, MMSE, and backward digit span) remained constant when the same analyses were conducted using raw scores (Supplementary Table 1).

Demographic and Clinical Data

Demographic and clinical characteristics at baseline and follow-up appear in Table 1. There were no statistically significant differences between groups in age (t (24) = −0.03, $p = 0.972$, $d = -0.01$) or years of education (t (24) = 1.68, $p = 0.104$, $d = 0.67$)). However, the interval between baseline and follow-up testing was longer for controls (MED = 26.50, IQR = 2.0) than for patients (MED = 24.00, IQR = 0.63; $U = 5.50$, $p < 0.001$, $r = -0.80$). Patients and controls did not show differences on CES-D (F (1, 24) = 0.091, $p = 0.766$, $\eta p2 = 0.004$), nor a group by time interaction effect (F (1, 24) = 2.709, $p = 0.113$, $\eta p2 = 0.101$).

Motor Performance

Regardless of the time point, SCA7 patients showed a slower articulation rate in PATA task (Fig. 1a) and a poorer motor performance in SARA (Fig. 1b), compared with controls (Table 2). It should be noted, however, that five patients were excluded because the progression of their ataxia prevented them to participate in the second MRI scanning; therefore, there is a bias of our results toward patients with smaller ataxia progression.

Cognitive Performance

Screening Tests

Cognitive deterioration in SCA7 patients at baseline and follow-up was revealed by significant main effects of the group for MMSE (Fig. 1c) and MoCA scores (Fig. 1d). Furthermore, MoCA scores of SCA7 patients also showed a significant decline over time (Table 2).

Verbal Memory

Regarding verbal working memory, SCA7 patients had a lesser span in backward digit task relative to controls

Table 1 Demographical and clinical features of controls and SCA7 patients

	Control group			SCA7 group		
	Baseline	Follow-up	Range	Baseline	Follow-up	Range
n	14	12		14	14	
Age	31.42 ± 11.37	33.75 ± 11.15	15–55	31.57 ± 10.50	33.64 ± 10.46	16–50
Sex (F/M)	4/8			5/9		
Years of schooling	10.63 ± 3.70		6–17	7.96 ± 4.24		2–17.5
Visit interval (months)		26.25 ± 1.28			24 ± .70	
CAG repeat length				49.14 ± 4.53		44–61
Disease evolution time (years)				6.35 ± 3.15		1–13
Depression scale (CES-D)	7.42 ± 5.35	11.16 ± 6.59	2–27	10 ± 9.39	8.57 ± 5.57	0–21
Gait ataxia onset (age in years)				26.21 ± 9.21		14–42
Visual deficit onset (age in years)				27.21 ± 11.62		15–48

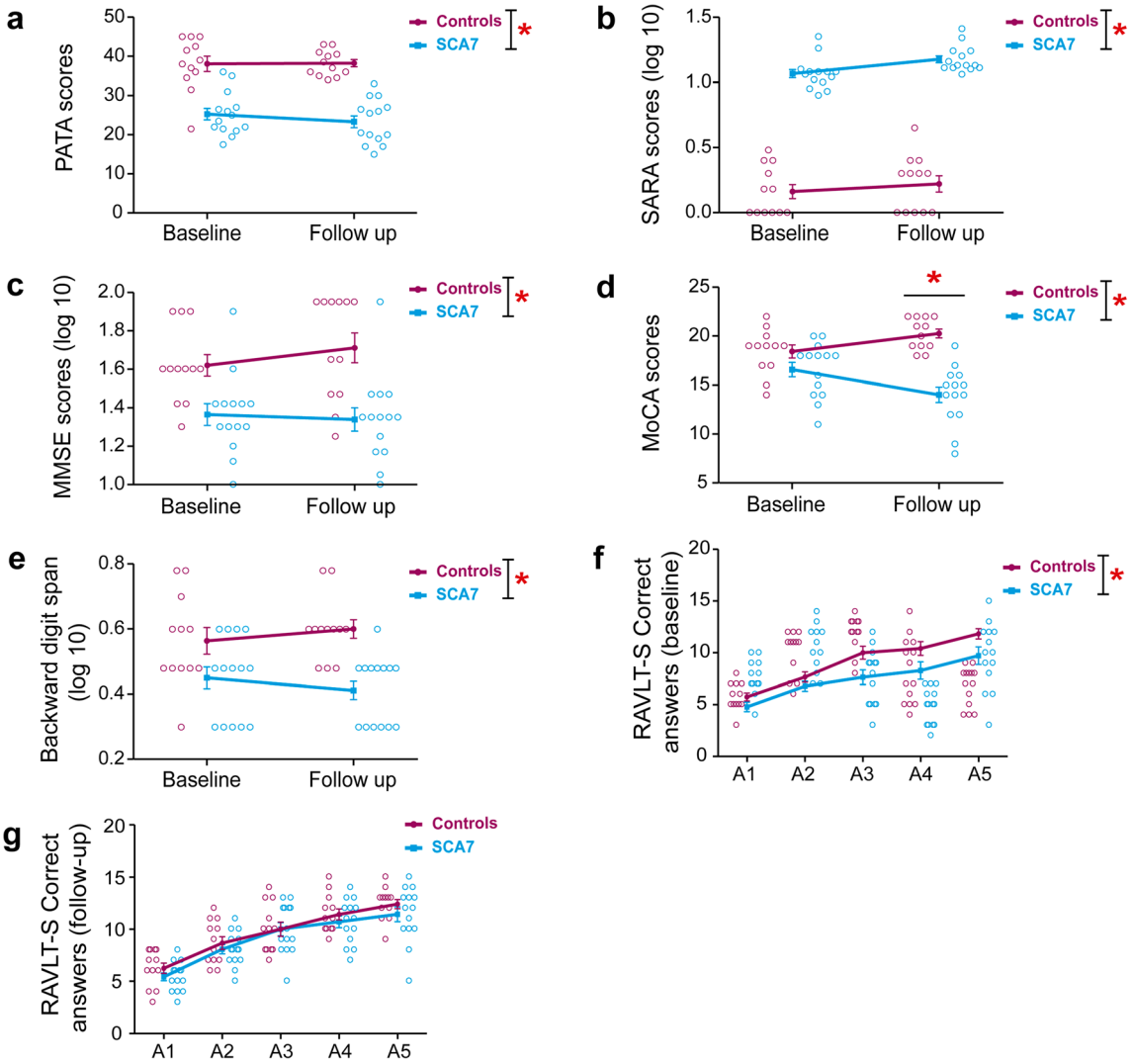

Fig. 1 Motor and cognitive tests showing significant longitudinal differences among controls and SCA7 patients. SCA7 patients showed a poor performance, reflected by a significant main effect of group, in **a** mean number of words correctly repeated in PATA test, **b** SARA scores, **c** MMSE scores, **d** MoCA scores, and **e** Backward digit span. SCA7 patients' MoCA scores (d) also showed a higher rate of deterioration (group × time interaction effect) at follow up. RAVLT-S learning curve was significantly slower in patients at baseline (**f**), but not at follow-up (**g**). Data are expressed as mean ± standard error of the mean. $*p < 0.05$ significant after FDR corrections

(Fig. 1e). Despite this main effect of group, result from SCA7 patients were not worsen from baseline to follow up (Table 2).

As shown in Table 2, the measures derived from RAVLT-S did not show statistically significant group or group-by-time interaction effects. Nevertheless, the analysis of the learning curve showed a statistically significant group-by-time interaction effect (F (1, 24) = 4.53, p = 0.044, $\eta p2 = 0.15$). Simple main effects revealed that SCA7 patients showed a slower curve than controls at baseline ($p = 0.036$; controls 9.13 ± 2.84; SCA7 7.44 ± 3.00; Fig. 1f), but not at follow-up ($p = 0.371$; controls 9.75 ± 2.87; SCA7 9.13 ± 2.98; Fig. 1g). These results could reflect an improvement of patients' memory strategies once they were exposed to the requirements of the task at baseline.

Verbal Fluency

There were no group differences in the initial status or in the linear slope (from baseline to follow-up) for the measures derived from semantic and phonemic fluency tasks (Table 3). However, there was a non-statistically significant tendency suggesting that patients were inclined to show reduced scores on total correct words (uncorrected $p = 0.077$) and number of switches (uncorrected $p = 0.044$) during the second evaluation (Table 3). This suggest an apparent but non-statistically significant faster decrease of semantic fluency scores over time.

Table 2 Longitudinal comparisons of motor, screening, and verbal memory tests among controls and SCA7 patients

	Control group		SCA7 group		Main effect of group				Group × time interaction effect			
	Baseline	Follow-up	Baseline	Follow-up	F value$_{(1, 24)}$	p value	q* value	η_p^2	F value$_{(1, 24)}$	p value	q* value	η_p^2
Motor performance												
PATA test	38.04 ± 6.82	38.20 ± 3.24	25.25 ± 5.54	23.32 ± 5.66	47.29	> 0.001	*0.050**	0.66	1.83	0.189	NS	0.07
SARA score	0.58 ± 0.73	0.87 ± 1.02	11.10 ± 3.83	14.50 ± 4.09	257.30	> 0.001	*0.025**	0.91	1.16	0.292	NS	0.04
Screening tests												
MMSE	25.92 ± 0.90	25.92 ± 1.38	24.21 ± 1.72	23.43 ± 2.10	15.49	0.001	*0.050**	0.39	1.99	0.171	0.050	0.08
MoCA (blind)	18.41 ± 2.31	20.25 ± 1.60	16.57 ± 2.77	14.00 ± 2.96	22.47	> 0.001	*0.025**	0.48	20.18	> 0.001	*0.025**	0.45
Verbal memory												
Backward digit span	3.83 ± 1.27	4.08 ± 0.99	2.93 ± 0.83	2.64 ± 0.63	13.58	0.001	*0.007**	0.36	2.95	0.098	NS	0.11
RAVLT-S												
Immediate memory span	5.75 ± 1.36	6.25 ± 1.76	4.79 ± 1.72	5.43 ± 1.40	2.62	0.118	0.014	0.09	0.06	0.800	NS	> 0.01
Learning rate	16.92 ± 5.98	17.50 ± 6.52	13.29 ± 8.40	18.50 ± 5.72	0.30	0.584	0.035	0.01	3.58	0.070	NS	0.13
Proactive interference	0.90 ± 0.33	0.93 ± 0.30	0.96 ± 0.28	0.77 ± 0.27	0.34	0.565	0.028	0.01	2.20	0.151	NS	0.08
Retroactive interference	0.82 ± 0.20	0.87 ± 0.09	0.77 ± 0.19	0.87 ± 0.18	0.13	0.716	0.050	> 0.01	0.63	0.432	NS	0.02
Forgetting rate	1.04 ± 1.49	0.89 ± 0.13	1.07 ± 0.33	1.03 ± 0.20	0.98	0.332	0.021	0.03	2.89	0.102	NS	0.10
Recognition memory	11.33 ± 3.14	11.33 ± 2.64	10.21 ± 3.99	11.07 ± 4.32	0.28	0.599	0.042	0.01	0.49	0.488	NS	0.02

* denotes significant q values (in italics)

Effect Size of Motor and Cognitive Tests Performance Rate Change

As shown in Table 4, SARA and MoCA change rates reached large effect sizes (above 0.90). However, the rest of the cognitive tests showed only weak to moderate effect sizes.

Neurodegeneration Analyses

Cross-sectional Gray Matter Analysis

VBM analysis revealed gray matter decrease in SCA7 patients in several cortical and cerebellar regions. The affected regions included the cerebellum, thalamus, pre- and postcentral gyri, medial and superior frontal gyri, superior and inferior parietal lobules, superior and medial temporal lobes, and medial occipital gyrus (Fig. 2. See Table 5 for a complete list of affected areas).

Whole-Brain Longitudinal Volumetric Analysis

SCA7 patients showed a statistically significant decrease of longitudinal gray matter density compared to controls after a period of 2 years. The affected areas included the brainstem; cerebellum; basal ganglia; thalamus; and orbitofrontal, mediotemporal, cingulate, and parahippocampal cortices (Fig. 3). Table 6 shows a complete list of the significant clusters, and their respective anatomical area (main and secondary), including the effect size of longitudinal gray matter degeneration.

Longitudinal Rate of Change Correlations Between Volumetric and Motor and Cognitive Measurements

Longitudinal changes in SARA scores were significantly correlated with the longitudinal volume loss in middle frontal, lingual, and superior frontal gyri. SARA score longitudinal deterioration also correlated with cortical thickness longitudinal loss in the superior frontal gyrus (Fig. 4 and Table 7).

Similar results were obtained between the longitudinal decline of MMSE scores and progressive volume loss in the right inferior and middle temporal gyri, the right entorhinal cortex, as well as progressive cortical thinning in the left anterior cingulate gyrus (Fig. 5 and Table 7). We also found statistically significant correlations between the longitudinal MoCA decline and the decrease of cortical thickness of right parahippocampal and paracentral cortices (Fig. 6 and Table 7). We did not find any statistically significant correlation between the rate of change of motor and cognitive measurements.

Discussion

Here, we performed a 2-year longitudinal characterization of the progression of the motor, cognitive, and brain deterioration in a cohort of SCA7 patients and a matched group of

Table 3 Longitudinal comparisons of semantic and phonemic verbal fluency tests among controls and SCA7 patients

	Control group		SCA7 group		Group (initial status)†					Group x time (linear slope)				
	Baseline	Follow-up	Baseline	Follow-up	Estimate (β)	Standard error	t value$_{(DOF)}$	p value	q^* value	Estimate (β)	Standard error	t value$_{(DOF)}$	p value	q^* value
Semantic fluency														
Total correct words	20.08 ± 5.40	22.67 ± 4.18	20.14 ± 2.98	17.21 ± 3.96	0.74	1.08	$t_{(37.38)} = 0.68$	0.499	NS	− 2.46	1.36	$t_{(51.28)} = -1.80$	0.077	0.025
Number of semantic clusters	3.92 ± 1.31	4.17 ± 1.31	3.21 ± 1.36	2.71 ± 1.59	0.03	0.39	$t_{(49.01)} = 0.08$	0.936	NS	− 0.83	0.61	$t_{(40.08)} = -1.36$	0.180	0.037
Mean cluster size	2.58 ± 0.73	3.02 ± 1.10	3.00 ± 1.61	2.35 ± 1.04	0.18	0.32	$t_{(45.20)} = 0.57$	0.569	NS	− 0.12	0.51	$t_{(38.99)} = -0.24$	0.814	0.050
Number of switches	11.25 ± 2.76	12.41 ± 3.87	14.50 ± 5.05	12.28 ± 4.90	2.01	1.01	$t_{(50.96)} = 1.99$	0.052	NS	− 3.24	1.56	$t_{(42.91)} = -2.07$	0.044	0.012
Phonemic fluency														
Total correct words	39.00 ± 10.96	45.33 ± 9.80	30.57 ± 9.63	32.57 ± 10.34	0.60	2.15	$t_{(51.59)} = 0.28$	0.782	NS	−2.50	3.29	$t_{(43.99)} = -0.76$	0.451	NS
Number of phonemic clusters	2.75 ± 2.42	3.08 ± 3.20	3.00 ± 1.57	2.71 ± 2.27	0.39	0.48	$t_{(51.74)} = 0.81$	0.421	NS	0.71	0.69	$t_{(45.28)} = 1.03$	0.307	NS
Mean cluster size	2.43 ± 0.89	2.12 ± 0.76	2.55 ± 0.64	1.94 ± 1.11	0.01	0.21	$t_{(26.88)} = 0.08$	0.940	NS	0.39	0.34	$t_{(27.56)} = 1.14$	0.261	NS
Number of switches	31.50 ± 7.80	38.08 ± 10.54	24.71 ± 11.82	27.14 ± 11.32	1.55	2.09	$t_{(47.03)} = 0.74$	0.461	NS	−4.96	2.93	$t_{(51.69)} = -1.70$	0.097	NS

Table 4 Longitudinal rate of change and effect size in SCA7 patients' behavioral tests

Behavioral test	Rate of change	Effect size index
SARA	0.014 ± 0.010	1.477
Verbal fluency		
Semantic verbal fluency		
Total correct words	− 0.006 ± 0.008	− 0.757
Number of clusters	− 0.001 ± 0.026	− 0.024
Mean cluster size	− 0.004 ± 0.019	− 0.233
Number of switches	− 0.005 ± 0.013	− 0.420
Phonemic verbal fluency		
Total correct words	0.004 ± 0.013	0.318
Number of clusters	− 0.005 ± 0.028	− 0.186
Mean cluster size	− 0.011 ± 0.019	− 0.562
Number of switches	0.006 ± 0.013	0.475
RAVLT-S		
Immediate memory span	0.010 ± 0.017	0.578
Learning rate	0.056 ± 0.98	0.574
Proactive interference	− 0.005 ± 0.016	−0.285
Retroactive interference	0.007 ± 0.013	0.548
Forgetting rate	0.000 ± 0.010	0.041
Recognition memory	0.014 ± 0.053	0.271
MoCA	− 0.006 ± 0.006	− 1.035
Backward digit span task	− 0.003 ± 0.009	− 0.308
PATA test	− 0.003 ± 0.004	− 0.769
MMSE	− 0.001 ± 0.003	− 0.514

healthy control participants. Our results suggest that progression of SCA7 is better quantified by measuring the atrophy longitudinal changes obtained by imaging analyses, followed by SARA and MoCA changes.

Our analyses show a significant longitudinal motor decline as assessed with SARA. Our results are consistent with multiple longitudinal studies analyzing the natural history progression of different SCAs using SARA, including SCA1, SCA2, SCA3, SCA6, SCA7, SCA17, and SCA 31 [41–45]. For example, our results showed that the SARA effect size index in SCA7 was 1.4, which is comparable to SCA1 (1.2) and SCA 3 (1.4), which have been reported previously [11]. However, a previous longitudinal study in a different SCA7 cohort showed an effect size of only 0.05 [10]. It is important to mention that SARA score deterioration is usually accompanied by the large brainstem and cerebellar volume loss, like those in SCA1, SCA2, SCA3, and in our SCA7 study, but not in patients with little volume loss, like in SCA6 [7, 10, 11, 46]. Further studies are needed to elucidate the possible reasons for the difference in the SARA score between the two SCA7 cohorts, i.e., our study and [10], despite having similar brainstem and cerebellar atrophy sizes.

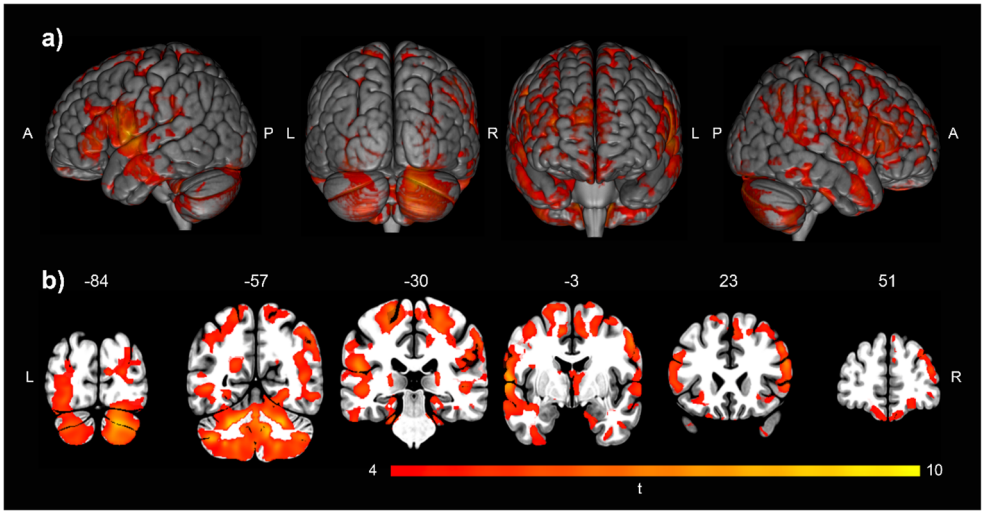

Fig. 2 Gray matter volume reductions in SCA7 compared to control group showed in three-dimensional rendering (**a**) and selected coronal sections overlaid on images from the MNI 152 atlas in neurological orientation (**b**). A, anterior; P, posterior,;L, left; R, right. Color bar indicates *t* values ($p < 0.05$)

Our results also showed that MoCA's longitudinal change was the only cognitive test with a large effect size deterioration in SCA7. We are currently unaware of any longitudinal SCA study using MoCA; however, there are studies in other neurodegenerative diseases suggesting that MoCA scores deterioration could be used as an important predictor of disease progression, including Parkinson's disease [47], mild cognitive impairment, and Alzheimer's disease [48]. These results suggest that, in future studies, it may be relevant monitoring MoCA scores to determine if other SCAs follow the same cognitive decline as assessed by this easy-to-apply screening test.

Imaging analyses showed a number of areas with significant group-by-time interactions suggestive of detectable brain atrophy during a 2-year period. The largest atrophy changes include areas within the temporal lobe, as well as the putamen, caudate, nucleus accumbens, cingulate, thalamus, brainstem, pons, and cerebellum. The analyses also showed significant correlations between the progression of degeneration and the progression of behavioral impairment. Notably, longitudinal thinning of the right parahippocampal and right paracentral gyri correlated with the MoCA score. Previous reports have shown parahippocampal atrophy correlations with deficits in cognitive tests, including RAVLT in SCA3 and SCA7 [8, 49], and verbal fluency in SCA7 [8]. These results show that the correlation of parahippocampal atrophy with cognitive tests declining found in cross-sectional studies can also be found during longitudinal analysis, suggesting that more research is needed to analyze the possible role of this structure in other SCAs where parahippocampal damage has been reported such as in SCA2 [50]. We are aware that there are three possible disadvantages of the MoCA test for the evaluation of patients with SCA7: (1) the individual cut-off points for MoCA are too lenient (e.g., backward digit range); (2) some tests are mini versions of the original test design (e.g., trails) that are not sensitive enough in this population for the mental flexibility that this test evaluates; and (3) errors in critical cognitive skills are hidden in the MoCA total score [51]. However, despite these disadvantages, we found statistically significant differences. It is possible that using tests such as the Schmahmann scale, which includes a short set of cognitive tests with sufficient sensitivity to detect the presence of cerebellar cognitive-affective syndrome and allows to selectively differentiate cerebellar patients from healthy people [51], would potentially increase the detection sensitivity of the cognitive deficits.

There are scarce longitudinal SCAs studies that include MRI analyses and clinical or cognitive tests [11, 52, 53]. These studies have found consistent atrophy in the cerebellum, brainstem, and pons as expected. They have also reported atrophy progression particular to each SCA, including for example the parahippocampal cortex, which correlated with global functioning deterioration in SCA17 [52]. It should also be noted that our findings related to the atrophy in the striatum resemble those previously reported in cross-sectional and longitudinal SCA studies, specifically in SCA1 and SCA3 [46, 53]. The only previous longitudinal study involving SCA7 patients that studied brain atrophy, analyzed only pons and cerebellar volumes in comparison with other SCAs (SCA1, SCA2, and SCA3) [10]. This previous SCA7 study also explored the relation of the progression of the pons and cerebellar degeneration with the decline in SARA and the Composite Cerebellar Functional Severity Score (CCFS). However, the authors did not report significant changes in SARA scores as

Table 5 Areas showing significant degeneration in the SCA7 group as shown in the Cross-sectional gray matter analysis

Anatomical location			Brodmann area	MNI coordinates (mm)			*t* value (local max)	*p*-corrected
				X	*Y*	*Z*		
Posterior lobe	Cerebellar tonsil	L		−34	−42	−44	4.01	0.999
Anterior lobe	Cerebellum	L		−22	−62	−32	9.72	0.999
Posterior lobe	Inferior semilunar lobule	R		18	−76	−38	11.44	0.999
Anterior lobe	Cerebellum	R		22	−62	−30	8.14	0.999
Frontal lobe	Precentral gyrus	L	4	−42	−12	46	4.78	0.998
Frontal lobe	Precentral gyrus	L	6	−60	0	8	7.93	0.999
Frontal lobe	Medial frontal gyrus	L	6	−12	−4	50	5.08	0.998
Frontal lobe	Superior frontal gyrus	R	6	26	8	66	4.57	0.997
Frontal lobe	Medial frontal gyrus	R	6	6	2	62	4.86	0.998
Frontal lobe	Precentral gyrus	R		50	22	34	5.38	0.999
Parietal lobe	Superior parietal lobule	L	7	−20	−50	68	4.48	0.998
Frontal lobe	Medial frontal gyrus	R	8	4	32	44	4.37	0.998
Frontal lobe	Superior frontal gyrus	R	8	6	40	46	4.45	0.998
Frontal lobe	Superior frontal gyrus	R	9	6	60	18	5.59	0.999
Frontal lobe	Superior frontal gyrus	L	9	−4	64	22	4.8	0.998
Frontal lobe	Middle frontal gyrus	L		−40	0	50	4.33	0.998
Frontal lobe	Medial frontal gyrus	L	10	−8	70	4	4.79	0.998
Frontal lobe	Middle frontal gyrus	R	10	40	60	−8	4.76	0.998
Frontal lobe	Superior frontal gyrus	R	10	34	58	18	5.5	0.998
Frontal lobe	Inferior frontal gyrus	L	45	−54	40	−2	5.21	0.999
Parietal lobe	Postcentral gyrus	R	2	60	−24	44	4.67	0.999
Parietal lobe	Postcentral gyrus	L	3	−20	−30	70	5.59	0.999
Parietal lobe	Inferior parietal lobule	R	40	52	−60	48	5.02	0.993
Parietal lobe	Supramarginal gyrus	L	40	−58	−38	36	4.34	0.999
Sub-lobar	Insula	L	13	−54	−32	20	7	0.999
Temporal lobe	Middle temporal gyrus	L	21	−64	2	−18	4.42	0.999
Temporal lobe	Superior temporal gyrus	L	21	−54	−26	−4	4.5	0.998
Temporal lobe	Middle temporal gyrus	R	21	58	8	−30	4.22	0.994
Temporal lobe	Superior temporal gyrus	R	22	60	12	−6	5.91	0.998
Temporal lobe	Fusiform gyrus	L	37	−50	−50	−12	4.31	0.998
Occipital lobe	Inferior occipital gyrus	L	18	−32	−90	−12	5.47	0.999
Occipital lobe	Middle occipital gyrus	R	19	30	−90	10	4.38	0.997
Occipital lobe	Middle occipital gyrus	R		60	−62	28	4.21	0.998
Thalamus	Pulvinar	R		24	−26	10	5.56	0.984
Thalamus	Pulvinar	L		−22	−24	8	5.97	0.997
Brainstem	Midbrain	R		8	−12	−22	4.57	0.992

discussed previously, or specific correlations between any structural decline and clinical scores [10].

SCA7 patients showed a poor mean performance in backward digit span and RAVLT-S learning curve compared to controls and a non-significant tendency toward impairment in semantic verbal fluency. Although these results seem to coincide with a previous cross-sectional study [8], the 2-year decline in our cohort did not reach statistical significance. It is likely that in longer longitudinal studies, the gradual deterioration of these cognitive scores would become evident.

A limitation of our study is that it relies on a few cases ($n = 14$). Taking the effect size of the rate of change in MoCA and SARA tests from our study, and a level of significance = 5%, power = 80%, $Z\alpha = 1.96$ and $Z\ (1\text{-}\beta) = 1.28$, and using the following formula $n = 2\ (Z\alpha + Z\ [1\text{-}\beta])2 \times SD2/d2$ [54, 55], we calculated a suggested minimum sample size of 21 for MoCA test

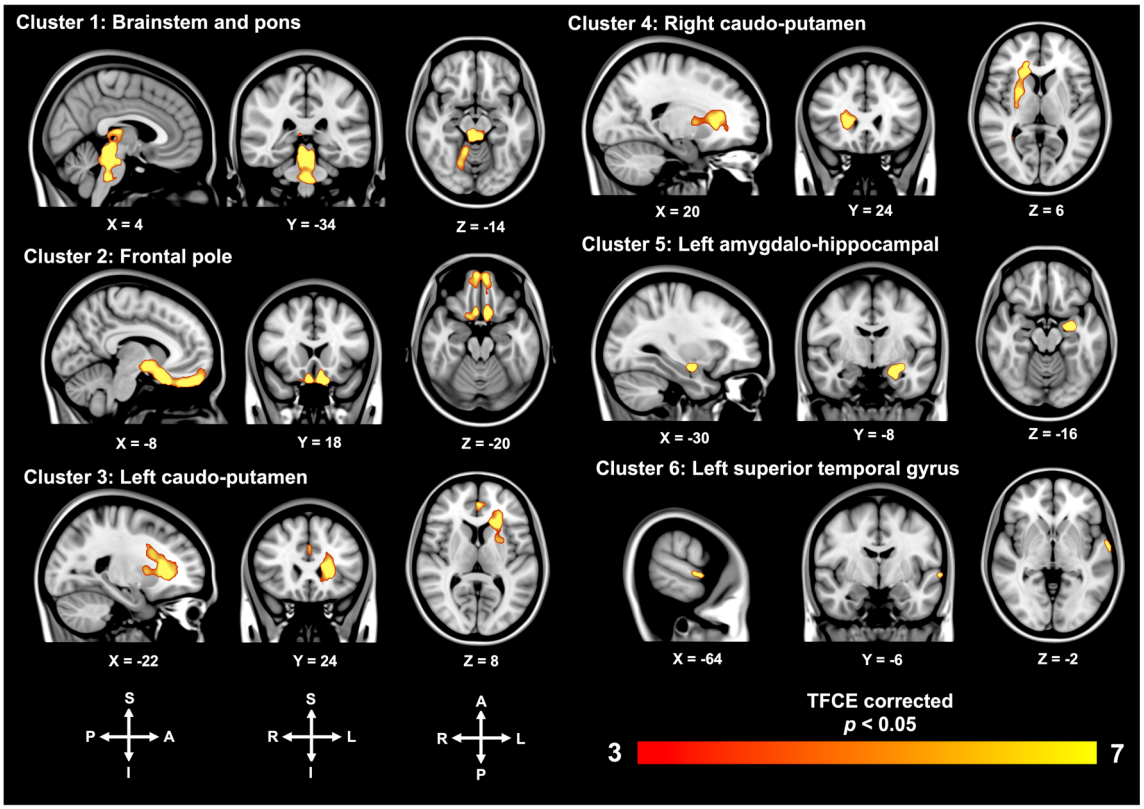

Fig. 3 Longitudinal GM change in SCA7 patients compared to healthy controls. The image shows significant clusters that demonstrate differences in atrophy progression given by interaction effect: time × group. Color scale bar indicates the *t* value ($p < 0.05$). Each panel shows a sagittal, coronal and axial view of the corresponding slices of the MNI anatomical template. Radiological orientation. TFC, threshold-free cluster enhancement; A, anterior; P, posterior; R, right; L, left; S, superior; I, inferior

and 10 for SARA test for a future clinical trial. Despite its high incidence in Mexico with respect to that in the world, SCA7 is still a rare disease; therefore, the sample size in this and in other studies has weak statistical power. Nonetheless, many of the results are highly significant suggesting that findings are robust. We must also acknowledge the high percentage of SCA7 patient's attrition, which is predictable given the increasing disability in this group. However, this infringes our assumption of missing data randomly and therefore, our estimates may be biased presumably toward less longitudinal change. Another limitation of our study is that it

Table 6 Areas showing significant longitudinal degeneration in the SCA7 group. VL = very large, H = huge

Cluster	Cluster size	*t* value (peak max)	MNI coordinates (mm)			Anatomical region included in the cluster		Effect size	Cohen's *d*
			X	*Y*	*Z*	Main	Secundary		
1	2086	20.2	4	− 34	− 14	Brainstem and pons.	Right thalamus and right cerebellum (I-IV, V, VI and Crus I)	1.171	VL
2	1918	18.1	− 8	18	− 20	Fontal pole	Bilateral orbitofrontal cortex	− 1.36	VL
3	1769	10.7	− 22	24	8	Left putamen and caudate.	Left paracingulate and anterior cingulate gyri	− 1.241	VL
4	1394	11.1	20	24	6	Right putamen and caudate	Right anterior cingulate gyrus	1.388	VL
5	208	16.4	− 30	− 8	− 16	Left amygdala, hippocampus	Left anterior parahippocampal gyrus	− 2.124	H
6	48	10.4	− 64	− 6	− 2	Left anterior and posterior superior temporal gyri	Anterior medial temporal gyrus	− 2.052	H

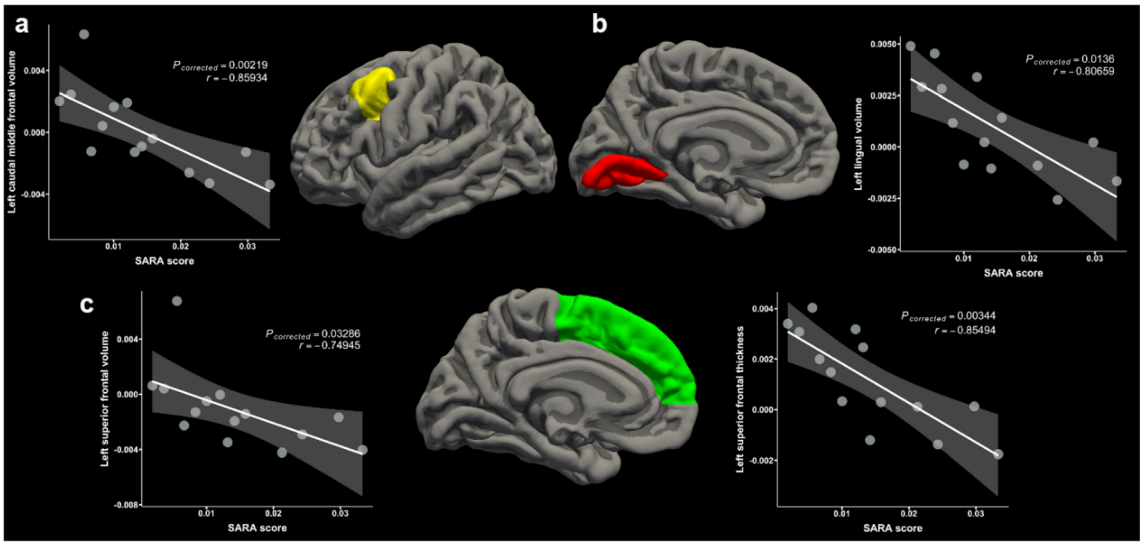

Fig. 4 Correlation of the SARA score longitudinal deterioration with cortical neurodegeneration in SCA7. Significant Spearman's rho correlations with volume loss in left caudal middle frontal gyrus in yellow (**a**), left lingual gyrus in red (**b**), and volume and cortical thinning in left superior frontal gyrus in green (**c**). All *p* values were FDR corrected

was focused on analyzing the progression of the disease once the onset of cerebellar neurodegeneration was recognizable at the clinical level and the cerebellar degeneration was noticeable at the structural level with MRI analysis. At this stage of degeneration, cognitive deterioration was not apparent. We are aware that the study of presymptomatic subjects would be ideal; however, in the communities that we have contacted, presymptomatic family members are not interested in knowing their molecular diagnosis or their neurological health status.

Our study of the follow-up of patients with SCA 7 for 2 years, reveals that the neurodegeneration of the brain could potentially be related to the emergence of cognitive impairment. It is important to remember that although ataxins are proteins preferentially expressed in the cerebellum, the distribution of their expression in the anterior brain is unknown for most of the SCAs. Differences in expression patterns could explain why in some SCAs there is a parallelism between the progression of motor and cognitive impairments and in some others does not. In the absence of immunohistochemical data, we believe that performing studies like ours for each type of SCA would contribute to shed light on this controversial issue.

Conclusion

Different approaches have been implemented as initial efforts to characterize the longitudinal progression in SCAs [56]. Here, we monitored a cohort of SCA7 patients during an interval of 2 years. Our results confirm previous studies in other SCAs showing that MRI-based structural markers can be used to detect the progression of the atrophy. However, our study found that SARA and MoCA are also good indicators of the progression of the disease. This is particularly relevant since it

Table 7 Areas showing longitudinal rate of change correlations between volumetric and motor and cognitive measurements in the SCA7 group

Clinical test	Anatomical region	*S*	Spearman's rho	R^2	*p* values*
SARA	Left caudal middle frontal volume	846	−0.8593407	0.5403	0.002188
	Left lingual volume	822	−0.8065934	0.5564	0.013766
	Left superior frontal volume	796	−0.7494505	0.346	0.033909
	Left superior frontal thickness	844	−0.8549451	0.6191	0.00344
MMSE	Right inferior temporal volume	781.82	−0.7182891	0.6973	0.024933
	Right middle temporal volume	790.15	−0.7365895	0.6152	0.024934
	Right entorhinal volume	848.43	−0.864692	0.6856	0.002236
	Left caudal anterior cingulate thickness	795.35	−0.7480272	0.6455	0.03598
MoCA	Right parahippocampal thickness	802	−0.7626374	0.5783	0.03852
	Right paracentral thickness	812	−0.7846154	0.5033	0.03851

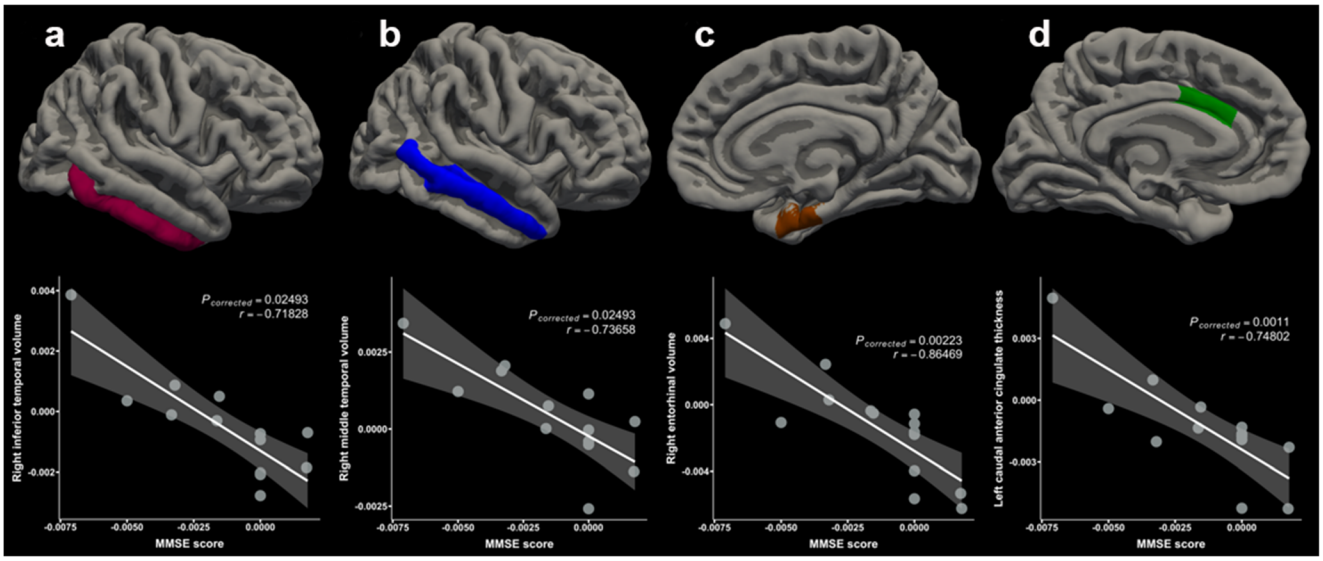

Fig. 5 Correlation of the MMSE score longitudinal deterioration with cortical neurodegeneration in SCA7. Significant Spearman's rho correlations with volume loss in right inferior temporal in maroon (**a**), right middle temporal in blue (**b**), and right entorhinal in brown (**c**) regions, and cortical thinning in caudal anterior cingulate in green (**d**) region. All *p* values were FDR corrected

has been suggested that for longitudinal and interventional studies, clinical scales like MoCA that are sensitive to disease progression and easy and fast to administer, should be favored, especially given the sociodemographic conditions of many of these groups of patients that preclude access to more advanced imaging facilities [56, 57].

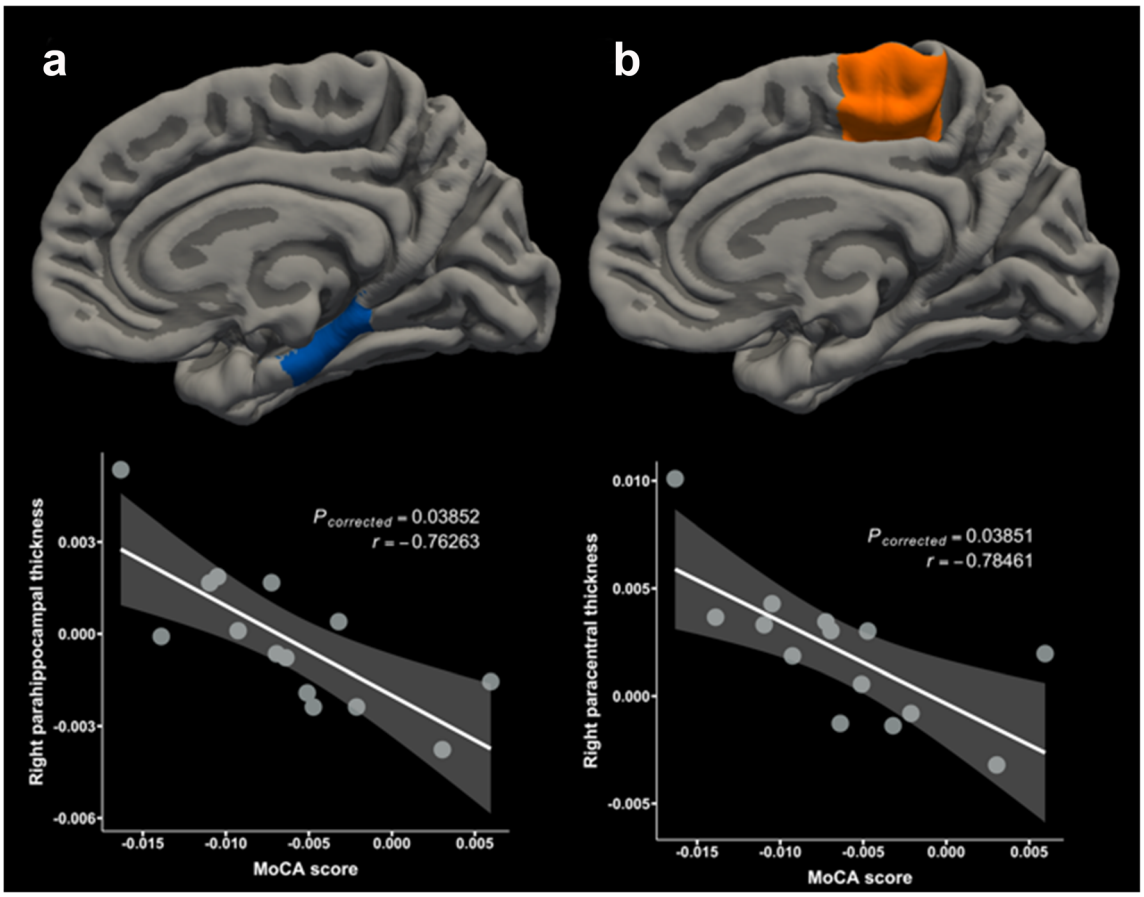

Fig. 6 Correlation of the MoCA score longitudinal deterioration with cortical neurodegeneration in SCA7. Significant Spearman's rho correlations with cortical thickness loss in right parahippocampal in blue (**a**) and right paracentral in orange (**b**). All *p* values were FDR corrected

Acknowledgments We are grateful to the SCA7 patients, their families, and volunteers for their valuable participation in this study.

Funding This study was supported in part by a doctoral scholarship CONACYT-326042 to Anabel Contreras Martínez (A.C.M.), it was also supported by CONACYT grant No. A1-S-10669 and PAPIIT-UNAM grant No. IN220019 to Juan Fernandez-Ruíz (JFR) and "Premio a la investigación interdisciplinaria en torno al Plan de restructuración estratégica del CONACYT 2018" to Luis Beltran-Parrazal.

Compliance with Ethical Standards

This study was approved by the human research ethics committee at the Faculty of Medicine at UNAM

Conflict of Interest The authors declare that they have no conflict of interest.

Ethical Approval Research and Ethics committee of the Faculty of Medicine of the Universidad Nacional Autónoma de México approved the study.

Statement of Informed Statement Written informed consent was obtained from each participant according to the Helsinki declaration.

References

1. Martin JJ, Van Regemorter N, Krols L, Brucher JM, de Barsy T, Szliwowski H, et al. On an autosomal dominant form of retinal-cerebellar degeneration: an autopsy study of five patients in one family. Acta Neuropathol. 1994;88:277–86. https://doi.org/10.1007/BF00310370.
2. David G, Abbas N, Stevanin G, Dürr A, Yvert G, Cancel G, et al. Cloning of the SCA7 gene reveals a highly unstable CAG repeat expansion. Nat Genet. 1997;17:65–70. https://doi.org/10.1038/ng0997-65.
3. Benomar A, Krols L, Stevanin G, Cancel G, LeGuern E, David G, et al. The gene for autosomal dominant cerebellar ataxia with pigmentary macular dystrophy maps to chromosome 3p12-p21.1. Nat Genet. 1995;10:84–8. https://doi.org/10.1038/ng0595-84.
4. Harding AE. Classification of the hereditary ataxias and paraplegias. Lancet. 1983;1:1151–5. https://doi.org/10.1016/s0140-6736(83)92879-9.
5. Johansson J, Forsgren L, Sandgren O, Brice A, Holmgren G, Holmberg M. Expanded CAG repeats in Swedish spinocerebellar ataxia type 7 (SCA7) patients: effect of CAG repeat length on the clinical manifestation. Hum Mol Genet. 1998;7:171–6. https://doi.org/10.1093/hmg/7.2.171.
6. Campos-Romo A, Graue-Hernandez EO, Pedro-Aguilar L, Hernandez-Camarena JC, Rivera-De la Parra D, Galvez V, et al. Ophthalmic features of spinocerebellar ataxia type 7. Eye (Lond). 2018;32:120–7. https://doi.org/10.1038/eye.2017.135.
7. Moriarty A, Cook A, Hunt H, Adams ME, Cipolotti L, Giunti P. A longitudinal investigation into cognition and disease progression in spinocerebellar ataxia types 1, 2, 3, 6, and 7. Orphanet J Rare Dis. 2016;11:82. https://doi.org/10.1186/s13023-016-0447-6.
8. Chirino A, Hernandez-Castillo CR, Galvez V, Contreras A, Diaz R, Beltran-Parrazal L, et al. Motor and cognitive impairments in spinocerebellar ataxia type 7 and its correlations with cortical volumes. Eur J Neurosci. 2018;48:3199–211. https://doi.org/10.1111/ejn.14148.
9. Alcauter S, Barrios FA, Díaz R, Fernández-Ruiz J. Gray and white matter alterations in spinocerebellar ataxia type 7: an in vivo DTI and VBM study. Neuroimage. 2011;55:1–7. https://doi.org/10.1016/j.neuroimage.2010.12.014.
10. Adanyeguh IM, Perlbarg V, Henry P-G, Rinaldi D, Petit E, Valabregue R, et al. Autosomal dominant cerebellar ataxias: imaging biomarkers with high effect sizes. Neuroimage Clin. 2018;19:858–67. https://doi.org/10.1016/j.nicl.2018.06.011.
11. Reetz K, Costa AS, Mirzazade S, Lehmann A, Juzek A, Rakowicz M, et al. Genotype-specific patterns of atrophy progression are more sensitive than clinical decline in SCA1, SCA3 and SCA6. Brain. 2013;136:905–17. https://doi.org/10.1093/brain/aws369.
12. Schmitz-Hübsch T, du Montcel ST, Baliko L, Berciano J, Boesch S, Depondt C, et al. Scale for the assessment and rating of ataxia: development of a new clinical scale. Neurology. 2006;66:1717–20. https://doi.org/10.1212/01.wnl.0000219042.60538.92.
13. Friedman LS, Farmer JM, Perlman S, Wilmot G, Gomez CM, Bushara KO, et al. Measuring the rate of progression in Friedreich ataxia: implications for clinical trial design. Mov Disord. 2010;25:426–32. https://doi.org/10.1002/mds.22912.
14. Nasreddine ZS, Phillips NA, Bédirian V, Charbonneau S, Whitehead V, Collin I, et al. The Montreal Cognitive Assessment, MoCA: a brief screening tool for mild cognitive impairment. J Am Geriatr Soc. 2005;53:695–9. https://doi.org/10.1111/j.1532-5415.2005.53221.x.
15. Tombaugh TN, McIntyre NJ. The mini-mental state examination: a comprehensive review. J Am Geriatr Soc. 1992;40:922–35. https://doi.org/10.1111/j.1532-5415.1992.tb01992.x.
16. Hebb D. Brain mechanisms and learning. In: Delafresnaye J, editor. Distinctive features of learning in the higher animal. New York: Oxford University Press; 1961. p. 37–46.
17. Jose P, Miranda J, Valencia RR. English and Spanish versions of a memory test: word-length effects versus spoken-duration effects. Hisp J Behav Sci. 2016. https://doi.org/10.1177/07399863970192005.
18. Malloy-Diniz LF, Lasmar VAP, de SR GL, Fuentes D, Salgado JV. The Rey Auditory-Verbal Learning Test: applicability for the Brazilian elderly population. Braz J Psychiatry. 2007;29:324–9. https://doi.org/10.1590/s1516-44462006005000053.
19. Troyer AK, Moscovitch M, Winocur G. Clustering and switching as two components of verbal fluency: evidence from younger and older healthy adults. Neuropsychology. 1997;11:138–46. https://doi.org/10.1037//0894-4105.11.1.138.
20. Soler J, Pérez-Sola V, Puigdemont D, Pérez-Blanco J, Figueres M, Alvarez E. Validation study of the Center for Epidemiological Studies-Depression of a Spanish population of patients with affective disorders. Actas Luso Esp Neurol Psiquiatr Cienc Afines. 1997;25:243–9.
21. Avants BB, Tustison NJ, Wu J, Cook PA, Gee JC. An open source multivariate framework for n-tissue segmentation with evaluation on public data. Neuroinformatics. 2011;9:381–400. https://doi.org/10.1007/s12021-011-9109-y.
22. Manjón JV, Coupé P, Martí-Bonmatí L, Collins DL, Robles M. Adaptive non-local means denoising of MR images with spatially varying noise levels. J Magn Reson Imaging. 2010;31:192–203. https://doi.org/10.1002/jmri.22003.
23. Ashburner J, Friston KJ. Voxel-based morphometry–the methods. Neuroimage. 2000;11:805–21. https://doi.org/10.1006/nimg.2000.0582.
24. Smith SM, Jenkinson M, Woolrich MW, Beckmann CF, Behrens TEJ, Johansen-Berg H, et al. Advances in functional and structural MR image analysis and implementation as FSL. Neuroimage. 2004;23(Suppl 1):S208–19. https://doi.org/10.1016/j.neuroimage.2004.07.051.
25. Smith SM. Fast robust automated brain extraction. Hum Brain Mapp. 2002;17:143–55. https://doi.org/10.1002/hbm.10062.

26. Good CD, Johnsrude IS, Ashburner J, Henson RN, Friston KJ, Frackowiak RS. A voxel-based morphometric study of ageing in 465 normal adult human brains. Neuroimage. 2001;14:21–36. https://doi.org/10.1006/nimg.2001.0786.
27. Hayasaka S, Nichols TE. Combining voxel intensity and cluster extent with permutation test framework. Neuroimage. 2004;23:54–63. https://doi.org/10.1016/j.neuroimage.2004.04.035.
28. Fischl B, Dale AM. Measuring the thickness of the human cerebral cortex from magnetic resonance images. Proc Natl Acad Sci U S A. 2000;97:11050–5. https://doi.org/10.1073/pnas.200033797.
29. Fischl B, Sereno MI, Dale AM. Cortical surface-based analysis. II: inflation, flattening, and a surface-based coordinate system. Neuroimage. 1999;9:195–207. https://doi.org/10.1006/nimg.1998.0396.
30. Fischl B, Liu A, Dale AM. Automated manifold surgery: constructing geometrically accurate and topologically correct models of the human cerebral cortex. IEEE Trans Med Imaging. 2001;20:70–80. https://doi.org/10.1109/42.906426.
31. Fischl B, Sereno MI, Tootell RB, Dale AM. High-resolution intersubject averaging and a coordinate system for the cortical surface. Hum Brain Mapp. 1999;8:272–84. https://doi.org/10.1002/(sici)1097-0193(1999)8:4<272::aid-hbm10>3.0.co;2-4.
32. Fischl B, Salat DH, Busa E, Albert M, Dieterich M, Haselgrove C, et al. Whole brain segmentation: automated labeling of neuroanatomical structures in the human brain. Neuron. 2002;33:341–55. https://doi.org/10.1016/s0896-6273(02)00569-x.
33. Fischl B, van der Kouwe A, Destrieux C, Halgren E, Ségonne F, Salat DH, et al. Automatically parcellating the human cerebral cortex. Cereb Cortex. 2004;14:11–22. https://doi.org/10.1093/cercor/bhg087.
34. Desikan RS, Ségonne F, Fischl B, Quinn BT, Dickerson BC, Blacker D, et al. An automated labeling system for subdividing the human cerebral cortex on MRI scans into gyral based regions of interest. Neuroimage. 2006;31:968–80. https://doi.org/10.1016/j.neuroimage.2006.01.021.
35. Ségonne F, Pacheco J, Fischl B. Geometrically accurate topology-correction of cortical surfaces using nonseparating loops. IEEE Trans Med Imaging. 2007;26:518–29. https://doi.org/10.1109/TMI.2006.887364.
36. Reuter M, Schmansky NJ, Rosas HD, Fischl B. Within-subject template estimation for unbiased longitudinal image analysis. Neuroimage. 2012;61:1402–18. https://doi.org/10.1016/j.neuroimage.2012.02.084.
37. Reuter M, Fischl B. Avoiding asymmetry-induced bias in longitudinal image processing. Neuroimage. 2011;57:19–21. https://doi.org/10.1016/j.neuroimage.2011.02.076.
38. Reuter M, Rosas HD, Fischl B. Highly accurate inverse consistent registration: a robust approach. Neuroimage. 2010;53:1181–96. https://doi.org/10.1016/j.neuroimage.2010.07.020.
39. Lancaster JL, Woldorff MG, Parsons LM, Liotti M, Freitas CS, Rainey L, et al. Automated Talairach atlas labels for functional brain mapping. Hum Brain Mapp. 2000;10:120–31. https://doi.org/10.1002/1097-0193(200007)10:3<120::aid-hbm30>3.0.co;2-8.
40. Risacher SL, Shen L, West JD, Kim S, McDonald BC, Beckett LA, et al. Longitudinal MRI atrophy biomarkers: relationship to conversion in the ADNI cohort. Neurobiol Aging. 2010;31:1401–18. https://doi.org/10.1016/j.neurobiolaging.2010.04.029.
41. Jacobi H, Bauer P, Giunti P, Labrum R, Sweeney MG, Charles P, et al. The natural history of spinocerebellar ataxia type 1, 2, 3, and 6: a 2-year follow-up study. Neurology. 2011;77:1035–41. https://doi.org/10.1212/WNL.0b013e31822e7ca0.
42. Tezenas du Montcel S, Charles P, Goizet C, Marelli C, Ribai P, Vincitorio C, et al. Factors influencing disease progression in autosomal dominant cerebellar ataxia and spastic paraplegia. Arch Neurol. 2012;69:500–8. https://doi.org/10.1001/archneurol.2011.2713.
43. Jacobi H, du Montcel ST, Bauer P, Giunti P, Cook A, Labrum R, et al. Long-term disease progression in spinocerebellar ataxia types 1, 2, 3, and 6: a longitudinal cohort study. Lancet Neurol. 2015;14:1101–8. https://doi.org/10.1016/S1474-4422(15)00202-1.
44. Nakamura K, Yoshida K, Matsushima A, Shimizu Y, Sato S, Yahikozawa H, et al. Natural history of spinocerebellar ataxia type 31: a 4-year prospective study. Cerebellum. 2017;16:518–24. https://doi.org/10.1007/s12311-016-0833-6.
45. Ashizawa T, Figueroa KP, Perlman SL, Gomez CM, Wilmot GR, Schmahmann JD, et al. Clinical characteristics of patients with spinocerebellar ataxias 1, 2, 3 and 6 in the US; a prospective observational study. Orphanet J Rare Dis. 2013;8:177. https://doi.org/10.1186/1750-1172-8-177.
46. Schulz JB, Borkert J, Wolf S, Schmitz-Hübsch T, Rakowicz M, Mariotti C, et al. Visualization, quantification and correlation of brain atrophy with clinical symptoms in spinocerebellar ataxia types 1, 3 and 6. Neuroimage. 2010;49:158–68. https://doi.org/10.1016/j.neuroimage.2009.07.027.
47. Kandiah N, Zhang A, Cenina AR, Au WL, Nadkarni N, Tan LC. Montreal Cognitive Assessment for the screening and prediction of cognitive decline in early Parkinson's disease. Parkinsonism Relat Disord. 2014;20:1145–8. https://doi.org/10.1016/j.parkreldis.2014.08.002.
48. Julayanont P, Brousseau M, Chertkow H, Phillips N, Nasreddine ZS. Montreal Cognitive Assessment Memory Index Score (MoCA-MIS) as a predictor of conversion from mild cognitive impairment to Alzheimer's disease. J Am Geriatr Soc. 2014;62:679–84. https://doi.org/10.1111/jgs.12742.
49. Lopes TM, D'Abreu A, França MC, Yasuda CL, Betting LE, Samara AB, et al. Widespread neuronal damage and cognitive dysfunction in spinocerebellar ataxia type 3. J Neurol. 2013;260:2370–9. https://doi.org/10.1007/s00415-013-6998-8.
50. Mercadillo RE, Galvez V, Díaz R, Hernández-Castillo CR, Campos-Romo A, Boll M-C, et al. Parahippocampal gray matter alterations in Spinocerebellar Ataxia Type 2 identified by voxel based morphometry. J Neurol Sci. 2014;347:50–8. https://doi.org/10.1016/j.jns.2014.09.018.
51. Hoche F, Guell X, Vangel MG, Sherman JC, Schmahmann JD. The cerebellar cognitive affective/Schmahmann syndrome scale. Brain. 2018;141:248–70. https://doi.org/10.1093/brain/awx317.
52. Reetz K, Lencer R, Hagenah JM, Gaser C, Tadic V, Walter U, et al. Structural changes associated with progression of motor deficits in spinocerebellar ataxia 17. Cerebellum. 2010;9:210–7. https://doi.org/10.1007/s12311-009-0150-4.
53. Mascalchi M, Diciotti S, Giannelli M, Ginestroni A, Soricelli A, Nicolai E, et al. Progression of brain atrophy in spinocerebellar ataxia type 2: a longitudinal tensor-based morphometry study. PLoS One. 2014;9:e89410. https://doi.org/10.1371/journal.pone.0089410.
54. Faul F, Erdfelder E, Lang A-G, Buchner A. G*Power 3: a flexible statistical power analysis program for the social, behavioral, and biomedical sciences. Behav Res Methods. 2007;39:175–91. https://doi.org/10.3758/bf03193146.
55. Gupta KK, Attri JP, Singh A, Kaur H, Kaur G. Basic concepts for sample size calculation: Critical step for any clinical trials! Saudi J Anaesth. 2016;10:328–31. https://doi.org/10.4103/1658-354X.174918.
56. Sarro L, Nanetti L, Castaldo A, Mariotti C. Monitoring disease progression in spinocerebellar ataxias: implications for treatment and clinical research. Expert Rev Neurother. 2017;17:919–31. https://doi.org/10.1080/14737175.2017.1364628.
57. Mercadillo RE, Galvez V, Díaz R, Paredes L, Velázquez-Moctezuma J, Hernandez-Castillo CR, et al. Social and cultural elements associated with neurocognitive dysfunctions in Sspinocerebellar ataxia type 2 patients. Front Psychiatry. 2015;6:90. https://doi.org/10.3389/fpsyt.2015.00090.